

# 3D-TOPOGRAPHY SIMULATOR FOR SEQUENTIAL PROCESSES

Masato Fujinaga

LSI R&D Lab., Mitsubishi Electric Corporation  
1 Mizuhara 4-chome, Itami, Hyogo 664, JAPAN  
Telephone: 0727-84-7325, Fax: 0727-82-7578

## ABSTRACT

This paper presents a 3D-topography simulator for sequential processes of photolithography, etching, deposition, and reflow. The basic algorithm is based on the calculation of the concentration of each material from the mass-conservation principle and on the representation of the material topography as contour surface: the area of constant concentration. It is straightforward for this algorithm to deal with multiple processes, multiple materials, and surface tension simultaneously.

## INTRODUCTION

The higher integration of circuits we aim at, the greater miniaturization of devices we have to realize. To cope with such a trend, the effects of edge topography and stress or tension become increasingly more important for the fabrication of ULSI circuits with multiple processes. So, it is required for 3D-topography simulators to be able to deal with multiple processes, multiple materials and stress or surface tension.

Several conventional models (the string model[1], the ray-tracing model[2], the cell removal model[3]) of topography expressions with the discontinuity at the material interface were introduced by R. E. Jewett, etc. The string model is adequate to analyze the stress or tension of elastic hard material, but it is difficult to maintain the mass-conservation principle in the mass transport mechanism. The cell model can be maintain the mass-conservation, but it is difficult to deal with stress or tension, as it can not explain oblique surfaces.

Although 3D-simulators using the conventional models have been presented [4,5,6] and are useful for individual processes, they don't have the generalization and the flexibility of dealing with mass-transport processes and surface tension in the three-dimensions simultaneously.

This paper introduces a 3D-topography simulator (3D-MULSS: Three-Dimensional Multi-Layer Shape Simulator) which can deal with mass-transport and surface tension simultaneously [7].

## MODEL

### 1. Material topography

When the interface of material is observed by the scattering of light or particle, the material topography strongly depends on the probe size of

the light or the particle. The observed value of material interface is given as the average of many material atoms or electrons in this probe size.  $C(x,y,z)$  is assumed to be the observed probability of material in the region between  $x$  and  $x + dx$ ,  $y$  and  $y + dy$ ,  $z$  and  $z + dz$ . If the light (or particle) is reflected to 'a constant direction', this average value  $C(x,y,z)$  can be differentiated by  $x$ ,  $y$ , and  $z$ , where  $(x,y,z)$  is position, and  $dx$ ,  $dy$ ,  $dz$  are assumed to be the dimensions of the probe. At this moment, as shown in Figs. 1 and 2, the material interface can be defined as follows:

$$|\text{grad}(C(x,y,z))| \gg 0 \text{ at the interface} \quad (1)$$

Then,  $-\text{grad}(C)$  is equivalent to the bisector direction between the incident and reflected directions and is the normal vector of the material surface.

If the thermal oscillation or the mean free path is considered in the solid or liquid, we find that surface tension or stress is an average force of many material atoms in a small region, too. So, the observed value of the interface is controlled by the thermal oscillation or mean free path, if the probe size is very small.

As described above, if a small area of the interface is considered,  $-\text{grad}(C)$  is the normal vector on the small surface. The surface is expressed as an area of the equal concentration, as illustrated in Fig. 3.

### 2. Transport of mass

Topography is changed by the mass-transport mechanism in the development of photoresist, etching, deposition, and reflow. Based on the mass-conservation principle, the  $C(x,y,z)$  is derived by solving the balance equation (2),

$$\partial C / \partial t + \text{div}(J) = G.R. \quad (2)$$

where  $C$  is the material concentration,  $J$  is the flux density of the material,  $G.R.$  is the generation-recombination rate, and  $t$  is the time.

As shown in Fig. 4, a way to solve Eq. (2), is to divide the area under investigation into small cells (small rectangular prisms), calculate the flux into or out of each small cell at short time intervals, and then derive the concentration in each small cell. For the etching and deposition processes, topography is dependent only on the flux into or out of surface cells of Fig. 4, directly. The topography is represented as contour surface at half of material density ( $C_0$ ). As the contour sur-

face is determined by a linear interpolation, the resolution is about one tenth of cell width. So, the simulation accuracy is about 10 times that of the cell model.

### 3. Etching model

This simulator has two isotropic etching models and one anisotropic etching model. The first isotropic etching model assumes that the etch rate is restricted by the surface chemical reaction, so the flux density of etched material is constant. The other isotropic model is restricted by the diffusion of etchant [8]. In the anisotropic etching model, it is assumed that the flux density of etched material is proportional to that of etchant which flows into each small local area, the mean free path of etchant is considered to be long enough, and the angular distribution of the etchant is a Gauss function. The surface shadowing is considered by calculating the solid angle.

### 4. Photolithography model

The topography of photoresist on a flat surface is determined by the 2D-image intensity [9], the inhibitor concentration of the photo chemical reaction [3], and the development of photoresist [10]. The development is assumed to be an isotropic etching restricted by the surface chemical reaction.

### 5. Al-sputter deposition model

Aluminum atoms are sputtered by Argon-ions hitting the Al-target. That Al-atoms are deposited on a wafer. An Argon-plasma is located between the Al-target and the wafer. The position of the wafer with respect to the disc of the Al-target (erosion area) is shown in Fig. 5. The erosion area of the Al-target is indicated in Fig. 5 by bold lines. The angular distribution of the sputtered Aluminum is given by  $\cos(\theta)$ . Because of the low gas pressure, it is assumed that the mean free path of Al-species is long enough to hit the wafer surface. The sticking coefficient of Al to the wafer surface is assumed to be 1. The surface shadowing is taken into account by calculating the solid angle, and the surface diffusion of Al is calculated [7].

### 6. Reflow model

The surface diffusion model [11] is used as the flux of BPSG. In this model, the molecules of BPSG flow from the position of high chemical potential is proportional to the reciprocal of the radius of the surface curvature.

## APPLICATIONS

Simulation results of the sequential processes are shown in Fig. 6. First the photolithography process is applied, for which it is assumed that the resist thickness is  $1 \mu\text{m}$ , the lithographic pattern is a square block of  $1 \mu\text{m}$ , the wave length is  $0.4358 \mu\text{m}$ , the numerical aperture is 0.54, the partial coherency is 0.5 and light is perfectly focused on the resist surface. There are small waves at the side wall of the simulated resist

which are caused by the standing wave effect. The second process step consists of the isotropic etching of oxide, which is restricted by the surface chemical reaction. This step is followed by an anisotropic etching, in which the angular distribution of etchant is assumed to be very small. Thereafter, the resist is removed. Finally, Aluminum is deposited by sputtering. In this case, surface diffusion is assumed to be severe (diffusion length =  $3 \mu\text{m}$ ). The total calculation time of these sequential processes is about 50 minutes with 15 MIPS CPU. In particular, it takes a long time to calculate the surface shadowing (35 minutes).

The reflow simulation of BPSG is shown in Fig. 7. The initial topography is given by the simulation of isotropic deposition of BPSG on a step of  $1 \mu\text{m}$  height, and the reflow time is 10 minutes. It is found that the initial surface is changed to a flat one.

## DISCUSSION

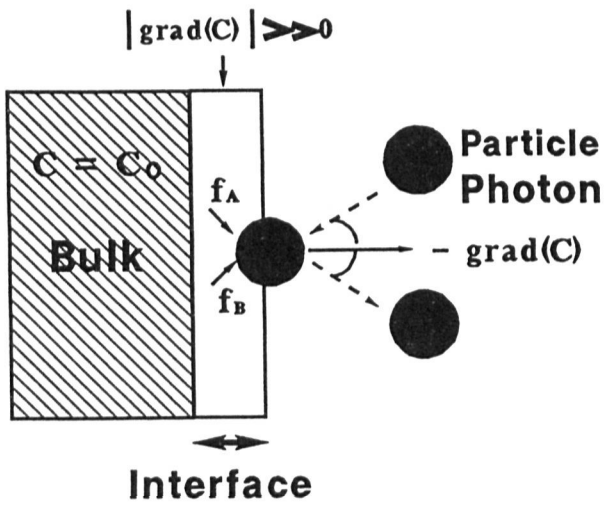
Since the basic algorithm of this topography simulator can be identified with that of impurity simulator, it can be expected in near future that a 3D-integrated process simulator for both topography and impurity will be realized.

## CONCLUSION

It is shown that material topography is expressed as a smooth contour surface, by considering the probe size of the observation. The 3D-topography simulator (MULSS) is based on this topography expression model and the principle of mass-conservation. The models and the application of MULSS are introduced and it is demonstrated that MULSS can simulate the sequential processes of photolithography, etching, deposition and reflow.

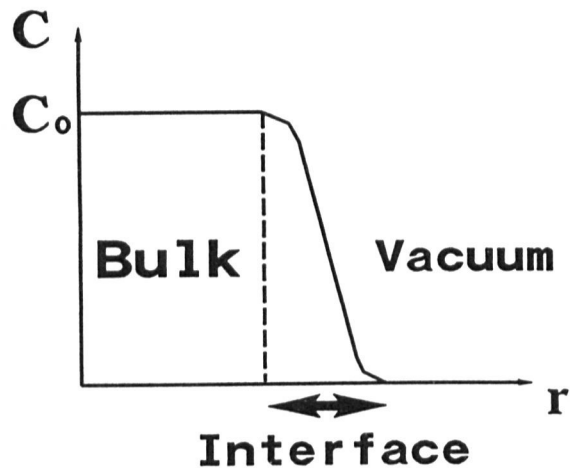
## REFERENCES

- [1] R.E. Jewett, et al : Polymer Engineering and Science, Vol.17, p.381, 1977.
- [2] P.I. Hagouel et al.: ACS Organic Coatings and Plastics Chemistry 170th. meeting, Chicago, p.298, 1975.
- [3] F.H. Dill et al.: IEEE Trans. Electron Devices vol.ED-22, p.456, 1975.
- [4] A.R. Neureuther, VLSI Process/Device Modeling Workshop, p. 82, Aug. 20-21, 1990. Kawasaki Japan.
- [5] A. Moniwa et al : IEEE Trans. Electron CAD, CAD-6, p. 431 (1987).
- [6] Y. Hirai et al : Symposium on VLSI Technology IEEE CAT. No. 87th 0189-1, p. 15, 1987.
- [7] M. Fujinaga, et al: IEDM'90 Technical Digest, p. 905, 1990.
- [8] M. Fujinaga et al.: IEEE Trans. Electron Devices, vol. 37, No.10, p.2183, 1990.
- [9] B.J. Lin : IEEE Trans. Electron Devices, Vol.ED-27, No.5, p.931, 1980.
- [10] D.J. Kim, et al: IEEE Trans. Electron Devices, Vol. ED-31, No.12, p.1730, 1984.
- [11] F. A. Leon : IEEE Trans. Electron CAD, Vol. 7, No.2, p. 168, 1988.



$f_A, f_B$ : Forces

Fig. 1 The essential property of interface



C : MATERIAL CONCENTRATION

Fig. 2 Bulk and interface

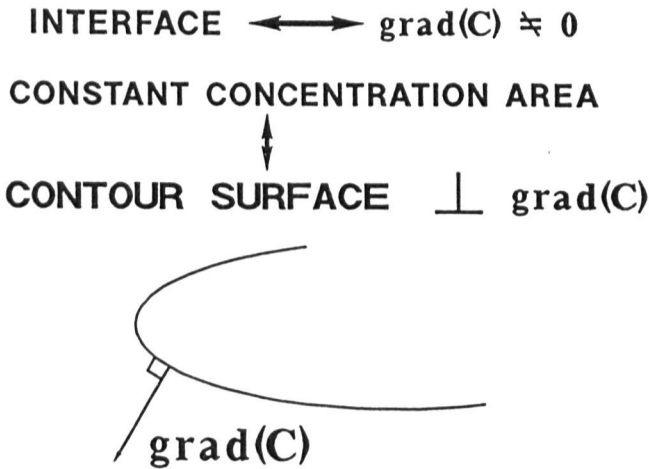


Fig. 3 Contour surface and grad(C)

|   |     |     |   |   |
|---|-----|-----|---|---|
| 1 | 0   | 0   | 0 | 0 |
| 1 | 0.1 | 0   | 0 | 0 |
| 1 | 1   | 0.2 | 0 | 0 |
| 1 | 1   | 0.3 | 0 | 0 |
| 1 | 1   | 0.5 | 0 | 0 |

Surface cell

Fig. 4 The example of topography expression

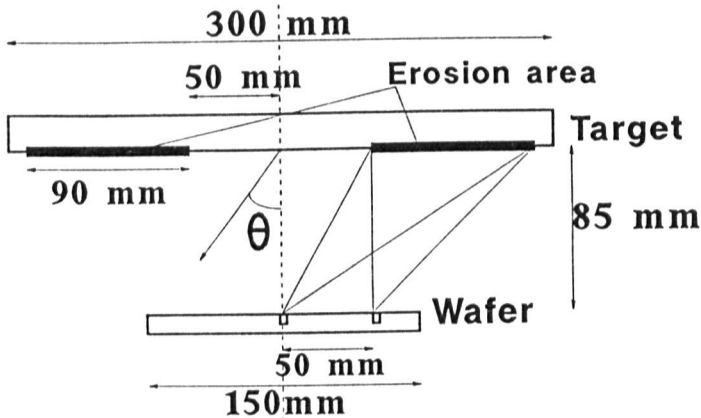


Fig. 5 Position of the wafer with respect to the target

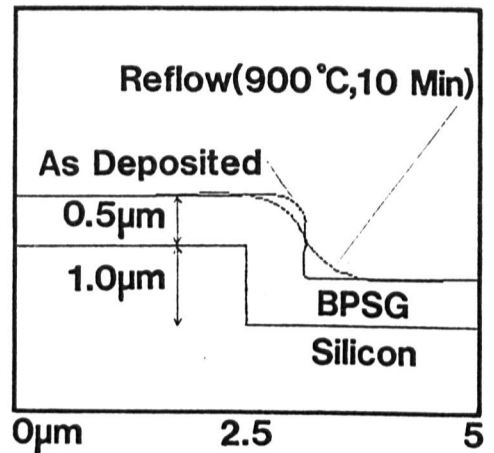


Fig. 7 Simulation of deposition and reflow

Fig. 6 Simulation of the sequential processes

